



The radial pressure gradient for turbulent flow in smooth pipes
by Charles Willis Greene

A thesis submitted to the Graduate Faculty in partial fulfillment of the requirements for the degree of
MASTER OF SCIENCE in Aerospace and Mechanical Engineering

Montana State University

© Copyright by Charles Willis Greene (1971)

Abstract:

An expression predicting a radial pressure gradient in turbulent smooth tube flow was derived. The radial pressure gradient for turbulent flow in smooth tubes was then measured experimentally for a range of Reynolds numbers from 57,000 to 484,000.

The results of the measurements show poor agreement with the predicted radial pressure gradient. The measured values were from four to thirteen times greater than the predicted values and indicate that the probe used did not measure the quantity which was, expected.

Statement of Permission to Copy

In presenting this thesis in partial fulfillment of the requirements for an advanced degree at Montana State University, I agree that the Library shall make it freely available for inspection. I further agree that permission for extensive copying of this thesis for scholarly purposes may be granted by my major professor, or, in his absence, by the Director of Libraries. It is understood that any copying or publication of this thesis for financial gain shall not be allowed without my written permission.

Signature

Charles W. Greene

Date

Dec. 15, 1970

THE RADIAL PRESSURE GRADIENT FOR
TURBULENT FLOW IN SMOOTH PIPES

by

CHARLES WILLIS GREENE

A thesis submitted to the Graduate Faculty in partial
fulfillment of the requirements for the degree

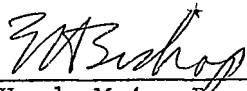
of

MASTER OF SCIENCE

in

Aerospace and Mechanical Engineering

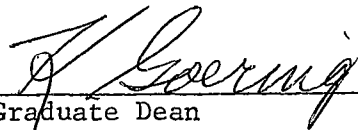
Approved:



Head, Major Department



Chairman, Examining Committee



Graduate Dean

MONTANA STATE UNIVERSITY
Bozeman, Montana

March, 1974

ACKNOWLEDGMENT

The author wishes to extend his sincere appreciation to Dr. Harry Townes under whose guidance this study was possible. Special thanks also are given to Dr. Ralph E. Powe whose assistance is deeply appreciated. Finally, the author's gratitude is also extended to Mr. Gordon Williamson for his skill at constructing the various probes used in this investigation.

TABLE OF CONTENTS

<u>Chapter</u>	<u>Page</u>
VITA	ii
ACKNOWLEDGMENT	iii
LIST OF FIGURES	v
NOMENCLATURE	vi
ABSTRACT	viii
I. INTRODUCTION	1
II. ANALYTICAL DEVELOPMENT	2
III. LITERATURE REVIEW	9
IV. EXPERIMENTAL SYSTEM	12
Apparatus	12
Procedure	17
V. EXPERIMENTAL RESULTS	21
VI. CONCLUSION AND RECOMMENDATIONS	30
APPENDIX I	31
LITERATURE CITED	33

LIST OF FIGURES

<u>Figure</u>		<u>Page</u>
1	Mean Velocity Distribution With Fluctuating Components	4
2	Axial Section of Pipe at an Arbitrarily Selected Zero Position	7
3	Schematic of Experimental System	13
4	Final Probe Design	15
5	Normal Stress Differences at $Re = 57,000$	24
6	Normal Stress Differences at $Re = 162,000$	25
7	Normal Stress Differences at $Re = 292,000$	26
8	Normal Stress Differences at $Re = 484,000$	27
9	Dimensionless Normal Stress Difference Between Pipe Wall and Center Line as a Function of Reynolds Number	28

NOMENCLATURE

<u>Symbol</u>	<u>Description</u>
D	Pipe diameter
P	Mean Pressure at any point in pipe
\bar{P}	Time average of mean pressure
r	Radial Coordinate
R	Pipe radius
Re	Reynolds number = $\frac{U_{avg} D}{\nu}$
T	Temperature
u*	Shear Velocity $(\tau_o/\rho)^{1/2}$
U	Mean velocity in axial direction
U_{avg}	Bulk mean velocity
U_{max}	Centerline mean velocity
u	Instantaneous value of fluctuating velocity in axial direction
\bar{u}	Time average value of instantaneous fluctuating velocity in axial direction
V	Mean velocity in radial coordinate direction
v	Instantaneous value of fluctuating velocity in radial direction
\bar{v}	Time average value of instantaneous fluctuating velocity in radial direction
W	Mean velocity in angular coordinate direction
w	Instantaneous value of fluctuating velocity in

<u>Symbol</u>	<u>Description</u>
	angular direction
\bar{w}	Time average value of instantaneous fluctuating velocity in angular direction
z	Axial Coordinate

<u>Greek Symbols</u>	<u>Description</u>
θ	Angular coordinate
ρ	Air density
ν	Kinematic viscosity
τ	Turbulent shear stress
τ_o	Wall shear stress
$\tau_{\theta\theta}$	Normal shear stress in the angular (θ) direction
κ	Bulk viscosity
∇	$\frac{\partial}{\partial r} + \frac{1}{r} \frac{\partial}{\partial r} + \frac{1}{r} \frac{\partial}{\partial \theta} + \frac{\partial}{\partial z}$
∇^2	$\frac{\partial^2}{\partial r^2} + \frac{1}{r} \frac{\partial}{\partial r} + \frac{1}{r^2} \frac{\partial^2}{\partial \theta^2} + \frac{\partial^2}{\partial z^2}$

<u>Subscripts</u>	<u>Description</u>
C	Refers to pipe centerline
W	Refers to pipe wall

ABSTRACT

An expression predicting a radial pressure gradient in turbulent smooth tube flow was derived. The radial pressure gradient for turbulent flow in smooth tubes was then measured experimentally for a range of Reynolds numbers from 57,000 to 484,000.

The results of the measurements show poor agreement with the predicted radial pressure gradient. The measured values were from four to thirteen times greater than the predicted values and indicate that the probe used did not measure the quantity which was expected.

CHAPTER I

INTRODUCTION

Turbulent flow in smooth tubes and over smooth boundaries has been studied quite extensively. As a result, theoretical studies, experimental data and semi-empirical theory have been developed which agree reasonably well. The theoretical expressions for turbulent flow in smooth tubes have also led to the development of an expression which predicts a radial pressure gradient in turbulent smooth tube flow. However, no experimental work has been done to verify the existence of this pressure gradient. Heretofore, this predicted radial pressure gradient has been considered negligible.

The purpose of this study was to experimentally measure the predicted radial pressure gradient in smooth tubes and to compare the measured values with the predicted values.

CHAPTER II

ANALYTICAL DEVELOPMENT

For turbulent pipe flow, a radial pressure gradient can be shown theoretically to exist. The Reynolds equations for incompressible flow in the three coordinate directions

$$U \frac{\partial U}{\partial z} + V \frac{\partial U}{\partial r} + \frac{W}{r} \frac{\partial U}{\partial \theta} = - \frac{1}{\rho} \frac{\partial P}{\partial z} - \left(\frac{\overline{\partial u^2}}{\partial z} + \frac{1}{r} \frac{\partial (r \overline{uv})}{\partial r} + \frac{1}{r} \frac{\partial (\overline{uw})}{\partial \theta} \right) + \nu \nabla^2 U \quad (2.1)$$

$$U \frac{\partial V}{\partial z} + V \frac{\partial V}{\partial r} + \frac{W}{r} \frac{\partial V}{\partial \theta} - \frac{W^2}{r} = - \frac{1}{\rho} \frac{\partial P}{\partial r} - \left(\frac{\partial \overline{uv}}{\partial z} + \frac{1}{r} \frac{\partial (r \overline{v^2})}{\partial r} + \frac{1}{r} \frac{\partial (\overline{vw})}{\partial \theta} - \frac{\overline{w^2}}{r} \right) + \nu \left(\nabla^2 V - \frac{V}{r^2} - \frac{2}{r^2} \frac{\partial W}{\partial \theta} \right) \quad (2.2)$$

and

$$U \frac{\partial W}{\partial z} + V \frac{\partial W}{\partial r} + \frac{W}{r} \frac{\partial W}{\partial \theta} + \frac{VW}{r} = - \frac{1}{\rho} \frac{\partial P}{\partial \theta} - \left(\frac{\partial (\overline{uw})}{\partial z} + \frac{\partial (\overline{vw})}{\partial r} + \frac{1}{r} \frac{\partial (\overline{w^2})}{\partial \theta} - \frac{2\overline{vw}}{r} \right) + \nu \left(\nabla^2 W + \frac{2}{r^2} \frac{\partial W}{\partial \theta} - \frac{W}{r^2} \right) \quad (2.3)$$

are obtained from the Navier Stokes equations by introducing the fluctuating velocity terms and time averaging each equation. The development of these expressions (2.1, 2.2, and 2.3) may be found in

such references as Hinze [1]¹ and Pai [4]. For the case of axially symmetric fully-developed pipe flow, the mean velocity components V and W are zero, all partial derivatives with respect to θ are zero because of symmetry and all velocity terms are independent of the axial component z . Therefore, the mean axial velocity component is a function of r only and the Reynolds equations reduce to

$$\frac{\partial(\overline{v^2})}{\partial r} + \frac{(\overline{v^2} - \overline{w^2})}{r} = -\frac{1}{\rho} \frac{\partial \overline{P}}{\partial r} \quad (2.4)$$

$$\frac{d(\overline{vw})}{dr} + \frac{2(\overline{vw})}{r} = 0 \quad (2.5)$$

and

$$\frac{d(\overline{vu})}{dr} + \frac{\overline{vu}}{r} = -\frac{1}{\rho} \frac{\partial \overline{P}}{\partial z} + \nu \left[\frac{d^2 U}{dr^2} + \frac{1}{r} \frac{dU}{dr} \right] \quad (2.6)$$

These equations can be simplified further by means of the following considerations. Figure 1 is a sketch showing the fluctuating velocity components and mean velocity profile in turbulent pipe flow. For any given point in the pipe, a fluctuation in the w component will result in no fluctuation in the u or v components. Therefore, it may be inferred that there can be no correlation of the v and w velocity fluctuations. If $\overline{vw} = 0$ then equation 2.5 is satisfied identically

¹Numbers in brackets refer to literature cited.

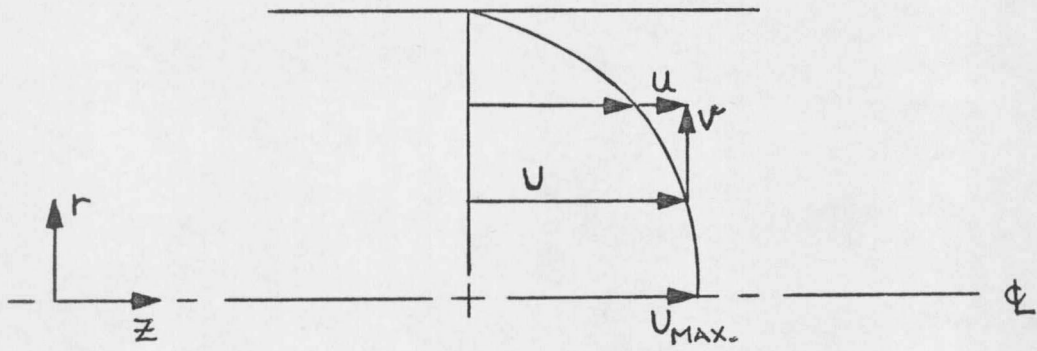


FIGURE 1. Mean Velocity Distribution With Fluctuating Components.

and of no further use.

Equation (2.4) may be rewritten as

$$-\frac{1}{\rho} \frac{\partial \bar{P}}{\partial r} = \frac{\partial \bar{v}^2}{\partial r} + \frac{(\bar{v}^2 - \bar{w}^2)}{r} \quad (2.7)$$

By integrating equation (2.7) with respect to r , the resulting equation is

$$\int_0^r \frac{\partial \bar{P}}{\partial r} dr = -\rho \int_0^r \left[\frac{\partial \bar{v}^2}{\partial r} + \frac{\bar{v}^2 - \bar{w}^2}{r} \right] dr \quad (2.8)$$

or

$$\bar{P} - \bar{P}_C = -\rho \left[(\bar{v}^2 - \bar{v}_C^2) + \int_0^r \frac{\bar{v}^2 - \bar{w}^2}{r} dr \right] + f(z) \quad (2.9)$$

where $f(z)$ is an unknown function of z .

The terms within the integral of equation (2.9) are functions only of the radial position r . Since the terms within the brackets of equation (2.9) are functions of r only, and since

$$\frac{\partial \bar{P}}{\partial z} = c \quad (2.10)$$

for fully developed flow then $f(z)$ must be

$$f(z) = C z \quad (2.11)$$

which can be taken as zero for an arbitrary axial position as in Figure 2.

Equation (2.9) then becomes

$$\bar{P} - \bar{P}_C = -\rho \left[\frac{\overline{v^2} - \overline{v_C^2}}{r} + \int_0^r \frac{\overline{v^2} - \overline{w^2}}{r} dr \right] \quad (2.12)$$

Equation (2.12) is then an equation for the mean static pressure of the fluid at any radial position minus the mean static pressure at the centerline. A similar expression for the mean static pressure at the wall minus the mean static pressure of the fluid at any radial position may be found by integrating equation (2.7) with respect to r again only between the limits of r and R . Following the same procedure as used in deriving equation (2.12) gives

$$\bar{P}_W - P = \rho \overline{v^2} - \rho \int_r^R \frac{\overline{v^2} - \overline{w^2}}{r} dr \quad (2.13)$$

Finally, by evaluating equation (2.13) at the centerline or by evaluating equation (2.12) at the wall, the theoretical expression for mean static pressure at the wall minus mean static pressure at the centerline may be found and is

$$\bar{P}_W - \bar{P}_C = \rho \overline{v_C^2} - \rho \int_0^R \frac{\overline{v^2}(r) - \overline{w^2}(r)}{r} dr \quad (2.14)$$

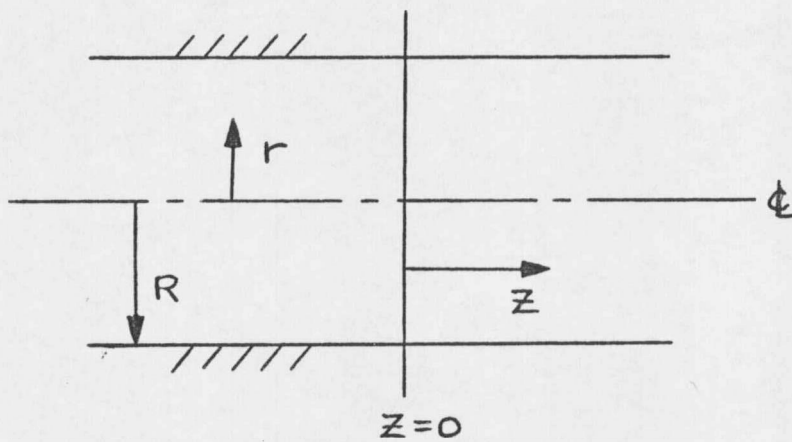


FIGURE 2. Axial Section of Pipe at an Arbitrarily Selected $z=0$ Position.

Equations (2.12), (2.13) and (2.14) are the theoretical expressions which imply the existence of a radial pressure gradient. Although it could be argued that the integral involving $\overline{v^2}$ and $\overline{w^2}$ is zero, the experimental data of Laufer [10], Gow [12], and others indicate that \overline{w} is always greater than \overline{v} except near the pipe centerline where they are equal. If \overline{w} is indeed greater than or at least equal to \overline{v} then equation (2.14) is always positive, which implies that the mean static pressure at the wall is greater than the mean static pressure at the centerline.

Equations (2.12), (2.13) and (2.14) were used to calculate the predicted curves for the radial pressure gradient by using the empirical data of Laufer [10] for values of $\overline{v^2}$ and $\overline{w^2}$.

CHAPTER III

LITERATURE REVIEW

A search of the literature was made to determine if any previous work had been done to measure experimentally the radial pressure gradient. That literature which was found included several technical papers and textbooks by Hinze [1], Schlichting [2], Longwell [3], and Pai [4].

The first source referred to was the ASME Codes [13]. These codes were reviewed in order to see what standards had been developed for the design of pitot-static probes or other applicable pressure measuring devices. This search revealed only one significant point which was that the static holes in the probe should be located at least eight support rod diameters upstream from the support rod. This length is sufficient to escape the effects of flow around a cylinder which could distort the true static pressure.

Regarding other applicable pressure measuring devices, Glaser [5] and Fechheimer [6] investigated two different types of pitot cylinders. Both of these designs utilized two holes located at a "critical angle" relative to one another. This "critical angle" is the angle at which the pressure distribution around a cylinder passes through the free stream static pressure value. However, the "critical angle" was different for each of the cases reported. In addition one can easily

show that the angle at which true static pressure occurs is a function of Reynolds number.

In 1959 R. Shaw [7] reported the influence of hole dimensions on static pressure measurements. His report stated that static pressure is influenced by the dimensions of a static pressure hole, and that an infinitely small hole would give the exact reading. A plot of pressure error (relative to a 0.0635 inch diameter reference hole) versus diameter of the static hole in inches was given for various average mean pipe velocities. The plots were extrapolated to zero diameter hole size and showed that the static holes of 0.0135 inches in diameter would give negligible error if no other contributing factors were present. The other factors included burrs around the outside and inside of the holes and deformed holes due to improper drilling.

Pai [8] presented a paper on turbulent flow in pipes in which he derived equation (2.14) for the radial pressure gradient. However, Pai's interpretation of the expression is different from this author's. Pai stated that the mean static pressure in the fluid will be greater than or equal to the mean static pressure on the wall for turbulent flow in circular pipes. The expression developed in this thesis is the same expression which Pai developed and existing data on turbulent flow indicates that the mean static pressure on the wall is greater than the mean static pressure in the fluid. It is not obvious how Pai

interpreted this expression.

In a paper by Brighton and Jones [9] the same expression (equation (2.14)) was derived for the radial pressure gradient. Their study was concerned with turbulent flow in annuli and they too interpreted the mean static pressure on the wall to be greater than the mean pressure in the fluid. However, they could not verify their theoretical results by experiment.

Laufer [10] has also reported on the structure of turbulence in fully developed pipe flow. In his paper he presented graphs of dimensionless fluctuating velocity components versus dimensionless radial position. These plots were for Reynolds numbers of 50,000 and 500,000 and showed no dependence of \bar{v} and \bar{w} on Reynolds number from the center of the pipe to about two-thirds of the way to the wall. This information was used in the development of expressions for \bar{v} and \bar{w} used in this thesis. These expressions for \bar{v} and \bar{w} are developed in digital computer programs which are available at Montana State University.

CHAPTER IV

EXPERIMENTAL SYSTEM

Apparatus

The experimental system shown schematically in Figure 3 was used throughout the investigation. Air was discharged from the centrifugal fan into the entrance section through eighty feet of flexible duct. Flow rates were controlled by a variable restriction on the inlet side of the fan. The entrance section, Figure 2 of Gow [12], contained a baffle plate and a series of screens to filter the air and dampen turbulence from the fan and return line. In the transition section, the cross sectional area of the entrance section was reduced from a four foot by four foot section to match the test pipe diameter of one foot. Seventy feet of one foot diameter aluminum irrigation pipe was used to insure fully developed flow at the test section. Suspension with adjustable brackets allowed for alignment of the pipe. The test section consisted of a three foot length of the same aluminum pipe coupled to the test pipe by a collar. The test section contained a static pressure piezometer ring and the experimental probe. The probe was mounted in the test section so that it could be moved radially from the center of the pipe to the wall.

The experimental probe was specially designed for this application

